Atomic-position resolution by quadrature-field measurement

Pippa Storey and Matthew Collett
Department of Physics, University of Auckland, Private Bag 92019, Auckland, New Zealand

Daniel Walls*
Joint Institute for Laboratory Astrophysics, University of Colorado, Boulder, Colorado 80309-0440
(Received 04 June 92)

An atom passing through a standing light field imparts a position-dependent phase shift to the field. By making a phase-sensitive measurement of the field, it is possible to resolve the atom's position to much less than the wavelength of the light. The field measurement results in the creation of virtual slits, and diffraction and interference phenomena may be observed. The phase measurements give *welcher Weg* information and enable "quantum-eraser" experiments to be realized.

PACS number(s): 32.80.-t, 03.65.Bz, 42.50.-p

I. INTRODUCTION

There is considerable activity in studying the mechanical effects of light on atoms [1]. It has been proposed that the deflection of atoms passing through a standing light wave may give a quantum-nondemolition measurement of the photon number in the light beam [2]. A recent experiment has demonstrated the optical Stern-Gerlach effect where an atom undergoes state-selective deflection when passing through a standing light wave [3].

Techniques for precise localization of the position of an atom have been developed. The channeling of atoms at the nodes of a standing wave using the gradient force has been demonstrated by Salomon *et al.* [4]. Measurement of atomic position with a resolution of 1.7 μm has been achieved by Thomas and co-workers [5] using spatially varying level shifts which enable one to correlate the position of the atom with its resonant frequency.

In this paper we describe a method to make a quantum measurement of the atom's position using the interaction with a standing light wave. A preliminary report on this method was given in Ref. [6]. When an atom passes through a standing light wave, information about the position of the atom is recorded in the phase of the field. By making a phase-sensitive measurement on the field, the atom's position may be determined to much less than the wavelength of the light. The resolving power of the scheme is found to be proportional to the amplitude of the radiation field.

If the atomic-position distribution is phase coherent before the interaction, the field measurement produces a quantum localization of the atom, rather than simply a classical position measurement. The atomic wave packet is altered, as if the atom had passed through a "virtual slit" (or slits). Interference from two such virtual slits is predicted, both in the near field and in the far field. The slits in this case are formed by the light, and the waves undergoing interference are matter waves.

Diffraction from a single virtual slit is also demonstrated. It is shown that as the width of the virtual slit is decreased, the diffraction pattern spreads out, as if a real physical slit were present. Because the slit width is adjusted by a local variable, the experiment is of a type suggested by Einstein, Podolsky, and Rosen (EPR).

The localization scheme is used to show how the availablity of *welcher Weg* information destroys interference in a double-slit experiment. The scheme also provides a very simple realization of a "quantum eraser."

II. LOCALIZATION SCHEME

An atom is passed through a standing wave in an optical cavity as indicated in Fig. 1. The strength of the atom's interaction with the light field depends on the atom's position relative to the nodes and antinodes of the cavity mode. Position information is extracted by making a phase-sensitive measurement on the field.

The transit time of the atom through the cavity is assumed to be much shorter than the lifetime of the cavity, which in turn must be much shorter than the time interval between successive atoms.

A. The Hamiltonian

The simplest possible coupling will be assumed; the atom is modeled as an ideal two-level system, and only a single mode of the radiation field is considered. Both the atom and the light field are treated quantum mechanically. The Hamiltonian for the combined atom-field system is

$$H = H_{\text{field}} + H_{\text{atom}} + H_{\text{int}} \tag{1}$$

where

$$\begin{aligned} H_{\text{field}} &= \hbar\omega_a(a^\dagger a + \tfrac{1}{2}), \\ H_{\text{atom}} &= \hbar\omega_o\sigma_z + \frac{p^2}{2m}, \\ H_{\text{int}} &= \hbar\cos(kx+\xi)(g^*\sigma_- a^\dagger + g\sigma_+ a). \end{aligned} \tag{2}$$

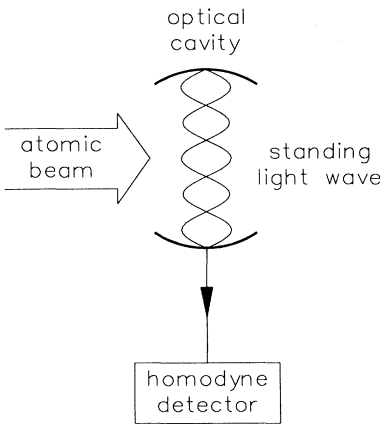

FIG. 1. The setup used for the position localization scheme.

Here a and $a^\dagger$ are the annihilation and creation operators for the cavity field, and σ_z, σ_-, and σ_+ are the internal atomic operators. ω_a and k are the frequency and wave number of the cavity mode. ω_0 is the atomic transition frequency, which is detuned from the cavity frequency by an amount $\Delta = \omega_0 - \omega_a$. $|g|$ is the coupling constant (equal to the one-photon Rabi frequency).

The transverse motion of the atom during its passage through the standing wave is assumed to be negligible (the Raman-Nath approximation). Under this condition the kinetic-energy term $p^2/2m$ may be omitted from the Hamiltonian.

When the atomic transition frequency is highly detuned from the cavity frequency, the probability is small that the field will induce an atomic transition between the ground and excited states. However, even for high detuning, the atom has a significant dispersive effect on the field. In effect the atom changes the refractive index of the cavity. The interaction is manifested as virtual transitions between the ground and excited states, in which the atom absorbs a photon from the field and then reemits it immediately by stimulated emission. If the atom is initially in its ground state, the population of the excited state will always be small and spontaneous emission can be neglected. This justifies the omission of atomic relaxation terms from the full Hamiltonian.

The effective Hamiltonian in the regime of large detuning, obtained by adiabatically eliminating the atomic coherences, is

$$H_{\text{eff}} = \hbar\omega_0\sigma_z + \hbar\omega_a a^\dagger a + 2\hbar\frac{|g|^2}{\Delta}\sigma_z a^\dagger a \cos^2(kx+\xi). \tag{3}$$

In a frame rotating at the cavity frequency ω_a the potential experienced by the atom as it passes through the standing wave is

$$V = 2\hbar\frac{|g|^2}{\Delta}\sigma_z a^\dagger a \cos^2(kx+\xi) + \hbar\Delta\sigma_z. \tag{4}$$

B. Initial conditions

Before the interaction with the atom, the field is assumed to be in a coherent state,

$$|\psi(0)\rangle_{\text{field}} = |\alpha\rangle \equiv D(\alpha)|0\rangle, \tag{5}$$

where $D(\alpha)$ is the displacement operator

$$D(\alpha) = \exp\left[\alpha a^\dagger - \alpha^* a\right] \tag{6}$$

and $|0\rangle$ is the vacuum state of the radiation field. The coherent state satisfies the eigenvalue equation

$$a|\alpha\rangle = \alpha|\alpha\rangle. \tag{7}$$

The atom is assumed to enter the cavity in its ground state with a transverse spread in position given by $\kappa(x)$. In order to observe interference effects, the atomic distribution must be phase coherent across its width, and the atom must therefore enter the cavity in a pure state

$$|\psi(0)\rangle_{\text{atom}} = \int dx\,\kappa(x)|x,g\rangle \tag{8}$$

where the ket specifies the position and internal state of the atom. To observe diffraction it is only essential to have phase coherence across the effective slit width; if this condition is satisfied, any departure from a pure state may be neglected. The initial state of the system is just the direct product of the initial field and atomic states.

C. System evolution

After an interaction time t, the combined atom-field state (in a frame rotating at frequency ω_a) is calculated by operating on the initial state with the evolution operator $U(t) = \exp(-iVt/\hbar)$,

$$|\psi(t)\rangle = \int dx\,\kappa(x) e^{-\frac{iVt}{\hbar}}|\alpha\rangle \otimes |x,g\rangle. \tag{9}$$

The evolution operator includes a factor $\exp\left[i\eta(x)a^\dagger a\right]$, where $\eta(x) = (|g|^2t/\Delta)\cos^2(kx+\xi)$ when evaluated over the atomic ket $|x,g\rangle$. This operator changes the phase of the field by an amount $\eta(x)$, which depends on the position of the atom (see Fig. 2):

$$e^{i\eta a^\dagger a}|\alpha\rangle = |\alpha e^{i\eta}\rangle. \tag{10}$$

If the atom passes through a node of the standing wave, no interaction occurs and the field is unchanged. However, if the atom passes through an antinode of the standing wave, the phase of the field is altered by an amount $|g|^2t/\Delta$.

Thus information about the position of the atom is recorded in the field, leaving the system in an entangled state of the atom and field

$$|\psi(t)\rangle = e^{\frac{i\Delta t}{2}}\int dx\,\kappa(x)\left|\alpha e^{i\frac{|g|^2t}{\Delta}\cos^2(kx+\xi)}\right\rangle \otimes |x,g\rangle. \tag{11}$$

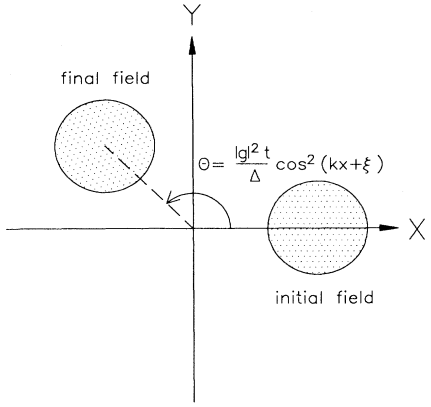

FIG. 2. An atom interacting with the standing wave at position x rotates the initial field state $|\alpha\rangle$ on the Wigner diagram, mapping it to the new state $\left|\alpha \exp\left[i\frac{|g|^2 t}{\Delta}\cos^2(kx+\xi)\right]\right\rangle$. X and Y denote the amplitude and phase quadratures of the field.

D. Measuring the field

The position of the atom relative to the nodes and antinodes of the standing wave can be deduced by measuring a phase-sensitive quantity such as the quadrature phase $X_\theta = ae^{-i\theta} + a^\dagger e^{i\theta}$. The observables $X_{\theta=0}$ and $X_{\theta=\pi/2}$ are referred to as the amplitude and phase quadratures, respectively, and are denoted more simply by X and Y. A quadrature phase measurement is directly realized using balanced homodyne detection [7]. The field leaks out of the cavity through the end mirror to produce a continuous sequence of values $\chi_\theta^{\rm out}(t)$. The continuous measurement of the cavity output is equivalent in its effect on the atomic state to an ideal instantaneous measurement $X_\theta = \chi_\theta$, where

$$\chi_\theta = \sqrt{2\gamma}\int_0^\infty d\tau\, e^{-\gamma\tau}\chi_\theta^{\rm out}(t_0+\tau). \tag{12}$$

Here γ is the cavity decay rate and t_0 is the time at which the atom passed through the standing wave. (The atom-field interaction time is assumed to be very short compared to the cavity lifetime.)

If the atom enters the cavity in a pure state, a determination of the field's phase after the interaction does not simply provide an indirect classical measurement of the atom's position; the field measurement collapses the atomic wave function, producing a quantum localization.

A quantum-mechanical treatment of the measurement process allows us to calculate the wave function of the atom after the field measurement. The measurement determines not only the probability of finding the atom at position x, but also the phase across the atomic distribution.

Suppose the field quadrature X_θ is measured, giving the result χ_θ. The state of the atom after the field measurement is found by projecting the system onto the eigenstate $|\chi_\theta\rangle$ of the quadrature operator X_θ

$$|\psi(t)\rangle_{\rm atom} = N\int dx\,\kappa(x)\left\langle \chi_\theta \left| \alpha e^{i\frac{|g|^2 t}{\Delta}\cos^2(kx+\xi)} \right\rangle |x,g\rangle, \tag{13}$$

where N is a normalization factor. The probability amplitude distribution of the atom after the measurement is simply

$$\psi_{\rm atom}(x,t) = N\kappa(x)\left\langle \chi_\theta \left| \alpha e^{i\frac{|g|^2 t}{\Delta}\cos^2(kx+\xi)} \right\rangle . \tag{14}$$

The position probability distribution $P(x|\chi_\theta)$ of the atom given that the value $X_\theta = \chi_\theta$ has been measured for the field is then

$$P(x|\chi_\theta) = |\psi_{\rm atom}(x,t)|^2 . \tag{15}$$

$P(x|\chi_\theta)$ satisfies the classical relation for conditional probabilities

$$P(x|\chi_\theta) = |N|^2 P(x)P(\chi_\theta|x), \tag{16}$$

where

$$P(x) = |\kappa(x)|^2 \tag{17}$$

is the overall probability of finding the atom at position x regardless of the field measurement, and

$$P(\chi_\theta|x) = \left|\left\langle \chi_\theta \left| \alpha e^{i\frac{|g|^2 t}{\Delta}\cos^2(kx+\xi)} \right\rangle\right|^2 \tag{18}$$

is the probability of measuring the value χ_θ for the field quadrature X_θ given that the atom is at position x. If the atom's position distribution is not phase coherent as it enters the cavity, the classical relation can still be used to obtain information about the position of the atom from the field measurement. In this case the process may be described as an indirect classical position measurement rather than a quantum localization. The atom leaves the cavity with a statistical position distribution, and no interference effects may be observed.

Calculation of Eq. (13) requires an expression for a quadrature phase eigenstate. $|\chi_\theta\rangle$ may be defined as a squeezed state in the limit of infinite squeezing

$$|\chi_\theta\rangle = \frac{1}{\sqrt[4]{2\pi}}\exp\left[-\tfrac{1}{2}(a^\dagger e^{i\theta} - \chi_\theta)^2 + \tfrac{1}{4}\chi_\theta^2\right]|0\rangle, \tag{19}$$

which satisfies the normalization condition

$$\langle\chi_\theta|\chi'_\theta\rangle = \delta(\chi_\theta - \chi'_\theta). \tag{20}$$

Using expression (19) in Eq. (13) gives the state of the atom after the field measurement $X_\theta = \chi_\theta$:

$$|\psi(t)\rangle_{\rm atom} = N\int dx\ \kappa(x)\frac{1}{\sqrt[4]{2\pi}} \times e^{-\left[(\alpha_1 - \frac{\chi_\theta}{2})^2 + i\alpha_2(\alpha_1 - \chi_\theta)\right]}|x,g\rangle, \tag{21}$$

where

$$\alpha_1 + i\alpha_2 \equiv \alpha e^{i[(|g|^2 t/\Delta)\cos^2(kx+\xi)-\theta]} \tag{22}$$

and N is a normalization factor.

III. MEASUREMENT OF THE ATOMIC POSITION

The resolution of the position measurement depends on the amplitude of the field and the value of the parameter $|g|^2t/\Delta$. This is the phase shift induced in the field by an atom located at an antinode of the standing wave. In all the graphs we will use $|g|^2t/\Delta = \pi$, and will take the initial field amplitude to be real.

A. Resolution

The localization scheme relies on measuring the phase of the field. The phase change induced by the atom depends on the vacuum light shift $(\hbar|g|^2/\Delta)\cos^2(kx+\xi)$ of the atomic ground state, and is independent of the number of photons in the cavity. However, the resolution with which a phase change can be detected depends on the amplitude of the field. The resolving power of the scheme is therefore proportional to $|\alpha|$, as is demonstrated in the following calculation.

The phase of the field after the interaction depends on whether the atom is located at a position x_0 or at a nearby position $x_0 + \delta x$. The resolution of the scheme is determined by the smallest position separation δx which will produce negligible overlap between the final field states.

The field is initially in a coherent state $|\alpha\rangle$, which has a fairly well-defined phase. If the atom is in a position eigenstate $|x_0\rangle$, the state of the field after the interaction will be

$$|\alpha(x_0)\rangle = |\alpha e^{i(|g|^2t/\Delta)\cos^2(kx_0+\xi)}\rangle. \tag{23}$$

Consider the region midway between a node and an antinode of the standing wave, where the phase induced on the field changes most rapidly with the position of the atom. This is the point at which maximum position resolution may be obtained. We may make the approximation $\cos^2(kx+\xi) \approx kx + \zeta$ for some ζ. Setting $|g|^2t/\Delta = \pi$, the overlap between the final field states which result if the atom is at positions $x = x_0$ and $x = x_0 + \delta x$ is

$$\begin{aligned}|\langle\alpha(x_0)|\alpha(x_0+\delta x)\rangle|^2 &\approx \left|\left\langle \alpha e^{i\pi[kx_0+\zeta]} \middle| \alpha e^{i\pi[k(x_0+\delta x)+\zeta]}\right\rangle\right|^2 \\ &= \exp\{2|\alpha|^2[\cos(\pi k\,\delta x) - 1]\} \\ &\approx \exp\left[-|\alpha|^2(\pi k\,\delta x)^2\right].\end{aligned} \tag{24}$$

The resolution of the measurement may be estimated from the exponent in the final expression

$$\delta x \sim \frac{1}{|\alpha|\pi k}. \tag{25}$$

The resolving power is therefore proportional to the amplitude of the field. We find that a field intensity of at least eight photons is required to resolve the atomic position to significantly less than a wavelength. This is the intensity which will be used in all the graphs except Fig. 13(b).

B. Testing the localization scheme

The position measurement properties of the scheme are characterized by the conditional probability $P(\chi_\theta|x)$. Evaluating this using Eq. (21), we obtain

$$P(\chi_\theta|x) = \frac{1}{\sqrt{2\pi}}e^{-2[\alpha_1(x)-(\chi_\theta/2)]^2}, \tag{26}$$

where $\alpha_1(x)$ is defined in Eq. (22). For a given position x, the probability of measuring $X_\theta = \chi_\theta$ has a Gaussian dependence on χ_θ.

The field measurement determines how close the atom is to a node or an antinode of the standing wave, but it cannot distinguish *which* node or antinode. The condi-

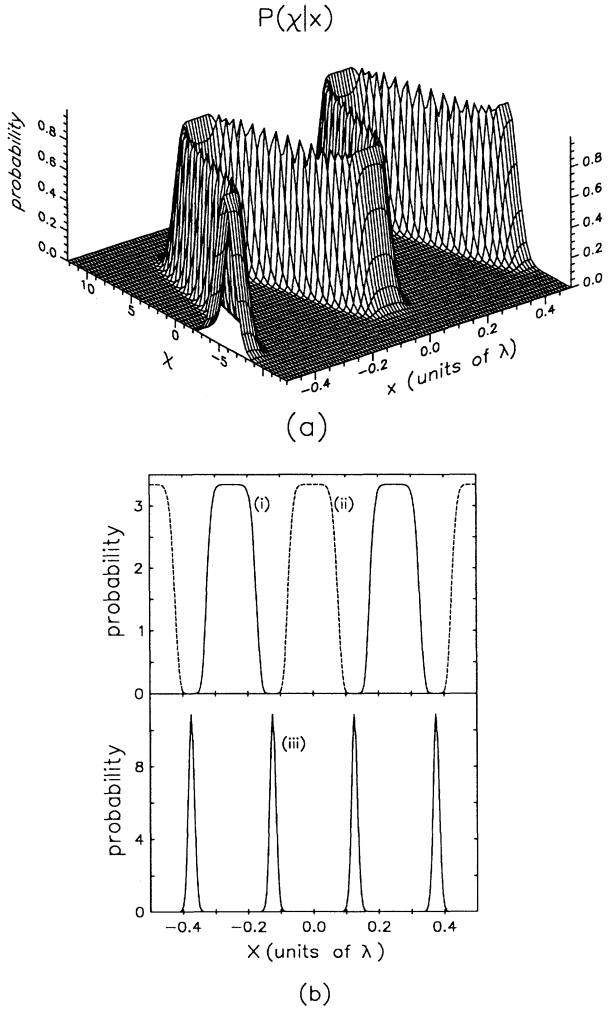

FIG. 3. (a) The conditional probability $P(\chi|x)$ of measuring $X = \chi$ given that the atom is located at position x. The field is coherent, with initial amplitude $\alpha = \sqrt{8}$. (b) The probability distribution of the atom after field measurements $X = 2\alpha$ (i), $X = -2\alpha$ (ii), and $X = 0$ (iii). It is assumed that no position information about the atom is known before it enters the cavity, and that $x = 0$ is an antinode of the standing wave.

tional probability function $P(\chi_\theta|x)$ repeats after every half wavelength of the standing wave, due to the periodicity of $\alpha_1(x)$.

Figure 3(a) shows the conditional probability $P(\chi|x)$ as a function of x and the value χ ($\equiv \chi_{\theta=0}$) of the amplitude quadrature. Suppose that the atom is not localized before it enters the cavity, that is it has a uniform position probability distribution $P(x) = \text{const}$. Its position distribution after a field measurement $X = \chi'$, determined from Eq. (16), is then $P(x|\chi') = |N|^2 P(\chi'|x)$, and is obtained by taking a "slice" through the plot $P(\chi|x)$ along the plane $\chi = \chi'$. The final position probability distributions for field measurements $X = \pm 2\alpha$ and $X = 0$ are shown in Fig. 3(b).

Better resolution is obtained for a field measurement $X = 0$ than for field measurements $X = \pm 2\alpha$. The field measurement $X = 2\alpha$ localizes the atom at a node of the standing wave, and the measurement $X = -2\alpha$ localizes the atom at an antinode of the standing wave. At both the nodes and antinodes of the standing wave the field intensity changes slowly with position, and poor resolution is obtained. For the field measurement $X = 0$ the atom is localized midway between a node and an antinode of the standing wave, where the field intensity changes rapidly with position and good resolution is obtained.

Using a squeezed field in the cavity [8] affects the resolution, but does not produce an overall improvement. If for example the initial field amplitude α is chosen to be real, then an amplitude squeezed field produces better resolution near the nodes and antinodes of the standing wave, but worse resolution midway between the nodes and antinodes. For a phase-squeezed field the opposite happens. Worse resolution is obtained near the nodes and antinodes of the standing wave, but better resolution is obtained midway between the nodes and antinodes.

IV. ATOMIC INTERFERENCE

If the spatial distribution of the atom is phase coherent as the atom enters the cavity, a measurement of the radiation field after the interaction produces a quantum collapse of the atomic wave function. Because of the periodicity of the standing wave, the resulting transverse position distribution may have multiple peaks. The light wave acts as a multiple slit, splitting a single atom into spatially separated atomic beams which subsequently interfere. This is a typical Young's interference experiment, except that the roles played by the light and matter are reversed. Interference of the atom may be seen both in the near field and in the far field [9].

A. Near-field interference

The field measurement does not only localize the atom in the transverse direction; it also introduces a spatially varying phase shift across the atomic distribution. This phase variation indicates deflection [3] and focusing [6,10] of the atomic beam. These effects can be understood from a semiclassical consideration of the light pressure forces acting on the atom. The potential seen by the atom as it crosses the standing wave is given by Eq. (4). Because the atom remains in the ground state throughout the interaction, and the intensity of the field is constant, we may make the substitutions

$$\sigma_z = -\tfrac{1}{2}, \qquad a^\dagger a = |\alpha|^2. \tag{27}$$

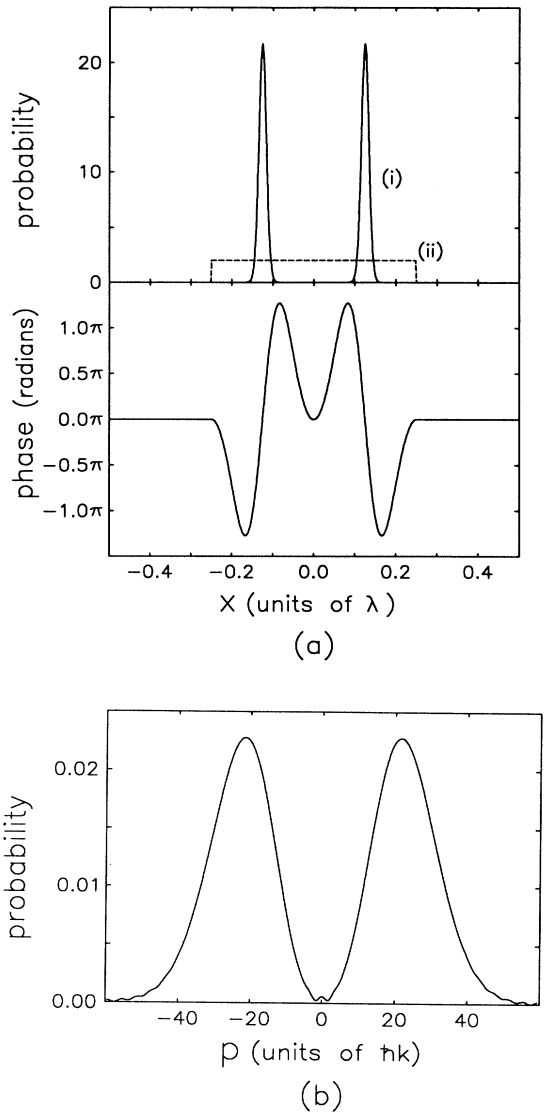

FIG. 4. (a) The atom enters the cavity in a "top hat" distribution of width $\lambda/2$ centred at an antinode of the standing wave (ii). The initial field amplitude is $\alpha = \sqrt{8}$. The field measurement $X = 0$ collapses the atomic distribution into two peaks (i). Immediately below is shown the phase across the atomic distribution after the field measurement. (b) The momentum distribution of the atom after the field measurement. No interference is seen because the two atomic beams are deflected in opposite directions and remain spatially separate in the far field.

The dipole force on the atom is then

$$f(x) = -\frac{dV}{dx} = -\hbar\frac{|g|^2}{\Delta}|\alpha|^2 k \sin\left[2\left(kx+\xi\right)\right]. \quad (28)$$

It is assumed that the atom's motion in the x direction is negligible during the interaction. The deflection of an atom interacting with the standing wave at position x for a time t is therefore given by

$$\Delta p = f(x)t = -\hbar\frac{|g|^2 t}{\Delta}|\alpha|^2 k \sin\left[2\left(kx+\xi\right)\right]. \quad (29)$$

The full quantum-mechanical treatment, performed in Sec. II, shows that unless the field is measured the state of the atom remains entangled with that of the field. However if the atom crosses the standing wave at position x, and the *most probable* value, namely, $\chi_\theta = 2\alpha_1$, is obtained from a measurement of the field quadrature, then the gradient of the phase induced across the atomic distribution corresponds exactly to the deflection of the atom calculated using semiclassical considerations. This phase shift is, from Eq. (21),

$$\phi(x) = -\alpha_2(x)\left[\alpha_1(x) - \chi_\theta\right]. \quad (30)$$

The gradient of the phase shift is

$$\phi'(x) = -\alpha_2'(x)\left[\alpha_1(x) - \chi_\theta\right] - \alpha_2(x)\alpha_1'(x) = -\frac{|g|^2 t}{\Delta}|\alpha|^2 k \sin\left[2\left(kx+\xi\right)\right], \quad (31)$$

and the deflection of the atomic beam is as given by Eq. (29).

Figure 3(b) shows that a field measurement $X = 0$ collapses the atomic distribution into a series of narrow peaks located midway between the nodes and antinodes of the standing wave. The phase variation induced across each of the peaks is approximately linear, indicating deflection of the atomic beams. The gradient of the phase variation is opposite across adjacent peaks, and the spatially separate "beams" of the atomic wave packet are deflected towards the antinodes of the standing wave. (For negative detuning deflection is towards the nodes.)

Suppose that before the interaction the atomic distribution is spread over half a wavelength, and is centered about an antinode of the standing wave. Then the field measurement $X = 0$ collapses the atomic distribution into only two peaks [see Fig. 4(a)]. The phase variation is opposite across each peak, so the two beams are deflected in different directions. In the far field the two beams are spatially separate and no interference is seen [Fig. 4(b)].

However, because the two atomic beams are deflected towards each other, interference may be expected in the near-field region where they cross. Figure 5(a) shows the propagation of the atomic probability distribution with time. The two beams converge on each other and produce interference in the region where they overlap. Figure 5(b) shows the atomic distribution in the interference region.

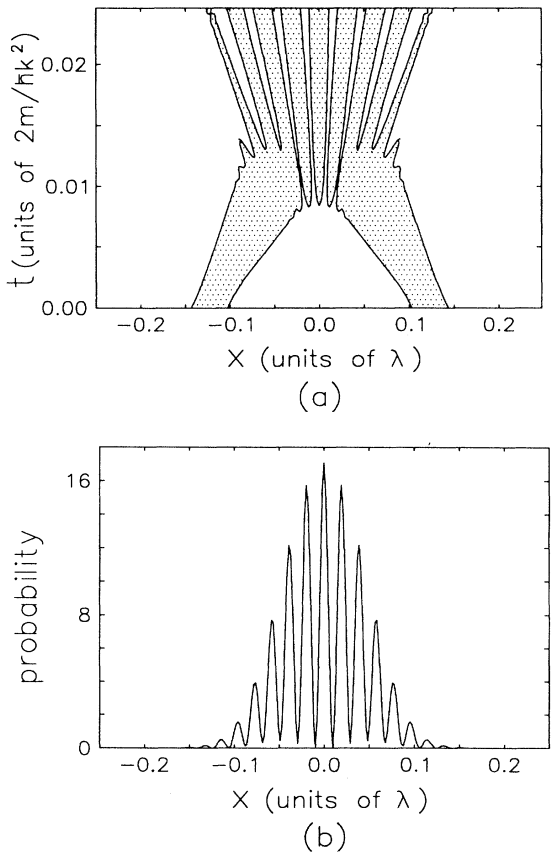

FIG. 5. (a) A contour plot of the propagation of the atomic probability distribution after the field measurement described in Fig. 4. For clarity only one contour is plotted and the regions of high probability are shaded. (b) The atomic probability distribution after a propagation time of $t = 0.015 \times 2m/\hbar k^2$.

B. Far-field interference

The field measurement $X = 0$ collapses the atomic distribution into a series of narrow peaks with opposite phase variation across adjacent peaks. Every alternate "beam" is deflected in the same direction, and interference may be expected between such beams in the far field.

Suppose the distribution of the atom before it enters the cavity is spread over three quarters of a wavelength. Then the measurement $X = 0$ collapses the atomic wave function into a distribution with three peaks [see Fig. 6(a)]. The two outer beams propagate in the same direction, and the central beam is deflected in the opposite direction. Interference is seen in the far field between the two outer beams [Fig. 6(b)]. The right half of the distribution is a typical double slit interference pattern, but in this case the double slit is produced by the measurement of the standing light wave, and the interference is of a single atom. The left half of the distribution is the diffraction pattern of the central peak.

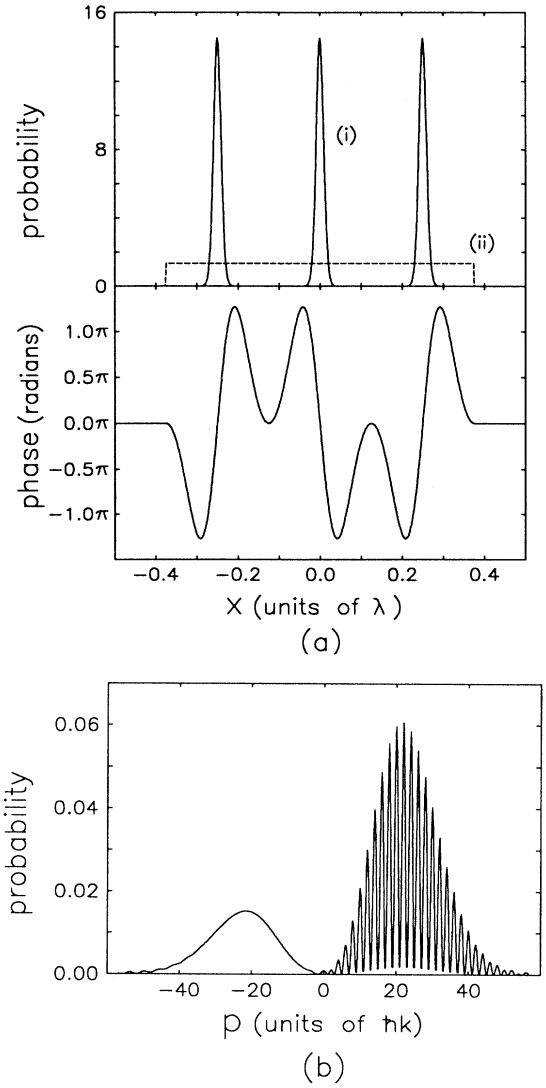

FIG. 6. (a) The atom enters the cavity in a "top hat" distribution of width $3\lambda/4$ (ii). The initial field amplitude is $\alpha = \sqrt{8}$. The field measurement $X = 0$ collapses the atomic distribution into three peaks (i). Immediately below is shown the phase across the atomic distribution after the field measurement. (b) The momentum distribution of the atom after the field measurement. Interference is seen between the two outer beams, which are deflected to the right. The left-hand half of the distribution shows the diffraction pattern of the central beam.

V. POPPER'S EXPERIMENT

In this section we suggest a method to implement an extension proposed by Popper [11] of the EPR gedanken experiment. Popper hoped to test whether knowledge of position is sufficient to create momentum uncertainty, as is contended under the Copenhagen interpretation, or whether the physical intervention of a measuring device is necessary to produce uncertainty. In the case of the Heisenberg microscope for example, one may think of the recoil due to the randomly scattered photon used to "see" the particle as having produced the momentum uncertainty. However, the EPR gedanken experiment points out the possibility of making an indirect measurement which involves no physical interaction of the particle under consideration with a measuring apparatus.

In Popper's proposed experiment, a source emits pairs of particles with opposite momenta. Detector arrays on each side of the source are wired to detect the pairs of particles in coincidence. A slit of adjustable width, placed in front of the detector array on the right, scatters the particles that pass through it. As the slit width is reduced, the range of scattering angles changes, and is monitored using the detector array. If a coincidence event is detected, it is known that the particle detected by the right-hand array passed through the slit. Because the particles are emitted from the source with opposite momenta, this provides indirect knowledge about the position of the left-hand particle. The Copenhagen interpretation predicts that, by virtue of our knowledge of the position of the left-hand particle, uncertainty is introduced into its momentum and the particle is scattered, as if from a "virtual slit." Popper argued that this virtual slit on the left should have the same width as the real one on the right. The same range of scattering angles should thus be detected by the left-hand array as by the right-hand array. In particular, when the slit is narrow enough, the range of detectors activated on the left should increase as the slit width is reduced. In fact, Popper's proposed experiment does not provide the crucial test of the Copenhagen interpretation for which it was designed [12]. Including the quantum uncertainties of the source (treated by Popper as precisely located) makes the virtual slit wider than the real one, and never narrow enough for diffraction effects to dominate.

A. Realizing Popper's test using the localization scheme

In previous sections it has been shown that knowledge about the position of an atom may be obtained indirectly by measuring the phase of a standing light wave with which it has interacted. The resulting localization of the atom can be regarded as the creation of a virtual slit. One way to adjust the width of the virtual slit is to change the phase of the field quadrature measured. This phase may be chosen after the interaction, when the atom and the light field have separated. The scheme is therefore an example of an EPR experiment, in which the phase of the field quadrature plays the role of the local variable.

The atom is injected into the cavity, with a narrow position distribution centered midway between a node and an antinode of the standing wave. Figure 7 indicates how the width of the virtual slit is adjusted. Suppose that the initial field amplitude is real, and that we choose to measure the amplitude quadrature X after the interaction. The most probable results from such a measurement would be close to the value $X = 0$, and would determine the phase of the field to within a small angle $\Delta\Theta_X$, allowing the position of the atom to be inferred with high

accuracy. An amplitude quadrature measurement therefore creates a narrow virtual slit. At the other extreme, suppose we choose to measure the phase quadrature Y. The most probable results would be close to the value $Y = 2\alpha$, and would determine the phase of the field only to within the large angle $\Delta\Theta_Y$, thereby providing a poor measurement of the atomic position. A phase quadrature measurement therefore produces a wide virtual slit.

The momentum variance of the atom after all possible amplitude and phase quadrature measurements are shown in Figs. 8(a) and 8(b), respectively. These curves are compared with the momentum variance when no field measurement is made. The probability distribution for the field quadrature measurements are indicated in each graph by the dashed line.

Figure 8(a) shows that if the amplitude quadrature is measured (producing a narrow virtual slit), then the atom is scattered over a wide angle. By comparison, Fig. 8(b) shows that if the phase quadrature is measured (producing a wide virtual slit), then, for any *probable* result of that measurement, the scatter is much less. This decrease in the scattering angle resulting from an increase in the slit width is exactly the behavior exhibited by real physical slits.

Virtual slits of intermediate widths may be obtained by setting the phase θ of the field quadrature X_θ to some value between 0 (an amplitude quadrature measurement) and $\pi/2$ (a phase quadrature measurement).

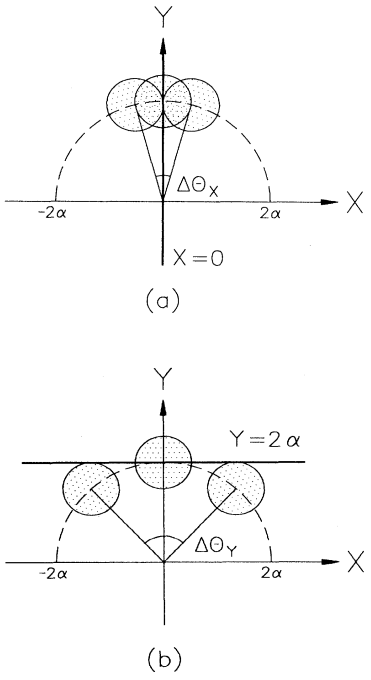

FIG. 7. (a) The measurement $X = 0$ of the amplitude quadrature determines the phase of the field to within the small angle $\Delta\Theta_X$, and thus provides a good measurement of the atom's position. (b) The measurement $Y = 2\alpha$ leaves an uncertainty $\Delta\Theta_Y$ in the phase of the field, and determines the atom's position with only poor resolution.

As the phase is decreased from $\pi/2$ to 0, the width of the virtual slits decreases, and the range of scattering angles increases smoothly [see curve (i) of Fig. 9]. The position variance and momentum variance plotted on the graph for a particular phase θ of the field quadrature are average variances, where the average is taken over all possible results of the field measurement, weighted by the probability of obtaining those results. The deviation from the minimum uncertainty relation $\Delta x\,\Delta p = \hbar/2$ occurs because of nonlinearity in the phase shift induced across the atomic distribution by the field measurement.

B. An improved realization of Popper's test

Another way to adjust the width of the virtual slit seen by the atom is to change the resolution of the field quadrature measurement. If knowledge about the value

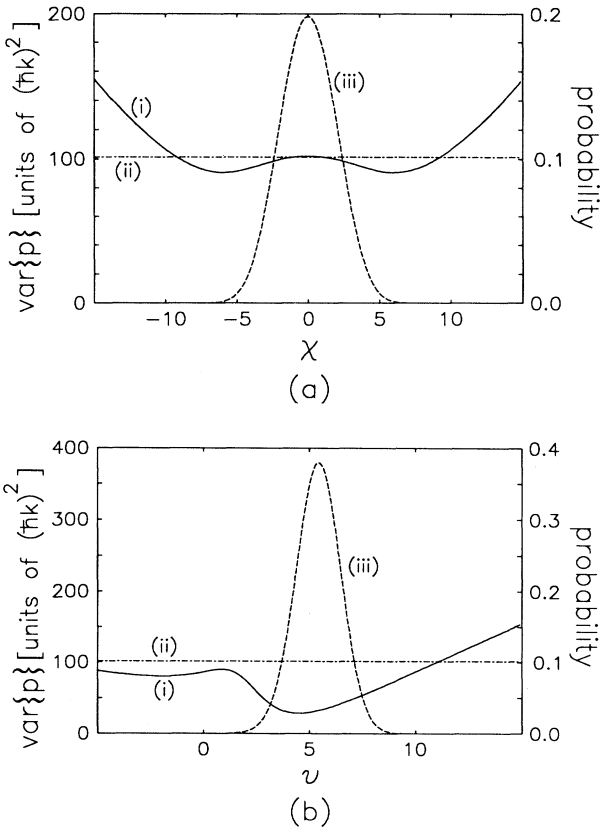

FIG. 8. (a) The momentum variance of the atom as a function of the value χ obtained from a measurement of the amplitude quadrature X (i). This is compared with the momentum variance when no field measurement is made (ii). The probability of measuring the value $X = \chi$ is shown by the dashed line (iii). (b) The corresponding functions after a phase quadrature measurement yielding the value $Y = \upsilon$. In both graphs the distribution of the atom before it enters the cavity is assumed to be Gaussian, with standard deviation $\sigma = 0.1\lambda/2\pi$, centered midway between a node and an antinode of the standing wave. The initial field amplitude is $\alpha = \sqrt{8}$.

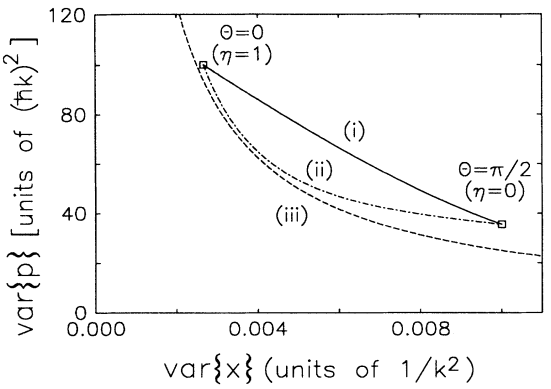

FIG. 9. The average momentum variance vs average position variance of the atom after measurements of the field quadrature X_θ, with θ varying from 0 to $\pi/2$ (i), and after amplitude quadrature measurements on the outputs of the beam splitter described in Sec. V B, with η varying from 0 to 1 (ii). These graphs are compared with the minimum uncertainty relation $\Delta x\,\Delta p = \hbar/2$ (iii). The initial parameters are the same as were used in Fig. 8.

of the field quadrature is imperfect, then information about the position of the atom is erased.

The resolution of the field quadrature measurement may be varied by splitting the field. Measuring the amplitude quadrature of both outputs of the beam splitter provides a simultaneous measurement of both the amplitude and phase quadratures of the cavity field [13], and in fact, realizes a measurement of the non-Hermitian operator $a\cosh r + a^\dagger \sinh r$ [14]. By adjusting the transmittivity η of the beam splitter, the resolution of the phase quadrature measurement increases, at the expense of the resolution of the amplitude quadrature measurement. By using this method to adjust the width of the virtual slit, instead of simply changing the phase of the field quadrature, we find that the momentum scatter of the atom increases as the atomic localization improves in much closer agreement with the minimum uncertainty relation.

The cavity field impinging on the beam splitter is described by the annihilation operator a. A vacuum field, described by the operator v, enters at the other face of the beam splitter. The outputs, described by the operators b and c, are related to the inputs by the equations

$$\begin{pmatrix} b \\ c \end{pmatrix} = \begin{pmatrix} \sqrt{\eta} & i\sqrt{1-\eta} \\ i\sqrt{1-\eta} & \sqrt{\eta} \end{pmatrix} \begin{pmatrix} a \\ v \end{pmatrix}. \tag{32}$$

If the transmittivity of the beam splitter is unity (or equivalently if the beam splitter is not present), then measurements of the amplitude quadratures X_b and X_c of the output fields constitute separate ideal measurements of the amplitude quadratures X_a and X_v of the input fields. As η is lowered, the resolution of the measurement of X_a decreases, and instead information is gained about the phase quadrature Y_a of the cavity field.

Using Eq. (11), we can write the state of the atom and cavity field after the interaction as

$$|\psi(t)\rangle = e^{\frac{i\Delta t}{2}} \int dx\, \kappa(x) |\alpha(x)\rangle \otimes |x, g\rangle \tag{33}$$

where

$$\alpha(x) \equiv \alpha e^{i(|g|^2 t/\Delta)\cos^2(kx+\xi)}. \tag{34}$$

The total system, which now includes the vacuum input to the beam splitter, may be described by

$$|\psi\rangle_{\text{total}} = e^{\frac{i\Delta t}{2}} \int dx\, \kappa(x) |0\rangle_v \otimes |\alpha(x)\rangle_a \otimes |x, g\rangle \tag{35}$$

where the subscripts a and v identify the cavity and vacuum inputs, respectively. The state of the atom after the values $X_b = \chi_b$ and $X_c = \chi_c$ have been measured for the beam splitter outputs is obtained by projecting the system onto the field state $|\chi_b\rangle_b \otimes |\chi_c\rangle_c$,

$$|\psi\rangle_{\text{atom}} = N \int dx\, \kappa(x) \{\langle\chi_b|_b \otimes \langle\chi_c|_c\} \times \{|0\rangle_v \otimes |\alpha(x)\rangle_a\} \otimes |x, g\rangle. \tag{36}$$

To evaluate the inner product between the initial and final field states, we express the output field states in terms of the input field operators

$$\begin{aligned} |\chi_b\rangle_b \otimes |\chi_c\rangle_c &= \frac{1}{\sqrt{2\pi}} e^{[-\frac{1}{2}(b^\dagger - \chi_b)^2 + \frac{1}{4}\chi_b^2]} e^{[-\frac{1}{2}(c^\dagger - \chi_c)^2 + \frac{1}{4}\chi_c^2]} |0\rangle_{\text{field}} \\ &= \frac{1}{\sqrt{2\pi}} e^{[-\frac{1}{2}(\sqrt{\eta}a^\dagger - i\sqrt{1-\eta}v^\dagger - \chi_b)^2 + \frac{1}{4}\chi_b^2]} e^{[-\frac{1}{2}(-i\sqrt{1-\eta}a^\dagger + \sqrt{\eta}v^\dagger - \chi_c)^2 + \frac{1}{4}\chi_c^2]} |0\rangle_{\text{field}}. \end{aligned} \tag{37}$$

The state of the atom after the field measurement is found by projecting the state $|\psi(t)\rangle_{\text{total}}$ onto the final field state given in Eq. (37),

$$|\psi\rangle_{\text{atom}} = N \int dx\, \kappa(x) e^{-\eta\left[\left(\alpha_1 - \frac{\chi_a}{2}\right)^2 + i\alpha_2(\alpha_1 - \chi_a)\right]} \times e^{-(1-\eta)\left[\left(\alpha_2 - \frac{v_a}{2}\right)^2 - i\alpha_1(\alpha_2 - v_a)\right]} |x, g\rangle, \tag{38}$$

where N is a normalization factor,

$$\chi_a = \frac{\chi_b}{\sqrt{\eta}}, \qquad v_a = -\frac{\chi_c}{\sqrt{1-\eta}}, \tag{39}$$

and α_1 and α_2 are defined in Eq. (22).

Adjusting the transmittivity of the beam splitter alters the resolution of the field quadrature measurement, and provides a method of adjusting the width of the virtual slit seen by the atom as it traverses the standing light

wave. If the transmittivity η of the beam splitter is increased from 0 to 1, then simultaneous measurements of the amplitude quadratures of the beam splitter outputs produce virtual slits of decreasing width. As the width of the virtual slit decreases, the range of scattering angles increases in good agreement with the minimum uncertainty relation [see curve (ii) of Fig. 9]. The position and momentum variances plotted on the graph for a particular transmittivity η are the variances averaged over all possible field measurements.

In principle the transmittivity of the beam splitter may be chosen locally after the atom-field interaction, when the atom can no longer be physically manipulated. Once again the scheme is an example of an EPR experiment, but this time the transmittivity of the beam splitter plays the role of the local variable.

The implementation of Popper's experiment considered in this subsection and the preceding subsection can be used to test whether mere knowledge of the position of the atom is sufficient to increase its momentum uncertainty.

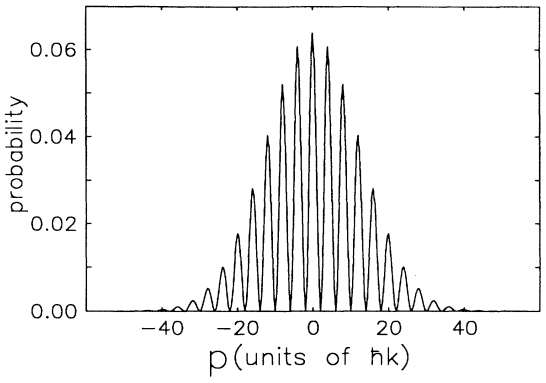

FIG. 11. In the absence of the cavity, the momentum distribution (identical to the far-field position distribution) exhibits the usual interference pattern. The slits are separated by a distance $\lambda/4$, and are each taken to have a Gaussian profile.

VI. *WELCHER WEG* INFORMATION

The position localization scheme presented in this paper can be used to determine which slit of a double-slit arrangement an atom has passed through. If one slit is located immediately ahead of a node of the standing-wave field and the other slit is located immediately ahead of an antinode, as shown in Fig. 10, then *welcher Weg* information (which-path information) is recorded in the phase of the field. It is found that as the position of the atom is determined with greater certainty, the visibility of the interference fringes decreases, in accordance with Bohr's principle of complementarity [15].

A. Loss of interference

In the absence of the cavity, the usual double-slit interference pattern is observed in the far field (see Fig. 11).

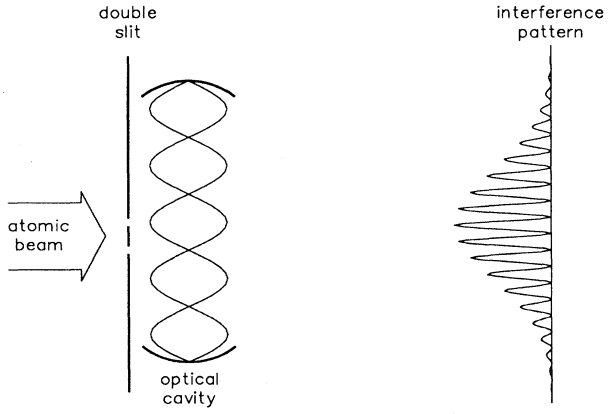

FIG. 10. The standing wave in an optical cavity placed immediately behind a double slit can be used to determine which slit an atom passed through.

Suppose now that the optical cavity is inserted behind the double slit. The cavity field is initially in a coherent state $|\alpha\rangle$, with α real. If the atom passes through the slit located at a node of the standing wave, no interaction occurs and the phase of the field is unaffected. However, if the atom passes through the slit located at an antinode of the standing wave, a phase shift of π is induced in the field [see Fig. 12(a)]. For a sufficiently high field intensity, a measurement of the amplitude quadrature X reveals the phase of the field, and determines which slit the atom passed through. The field measurement collapses the wave function of the atom so that its position distribution is localized about that slit. Consequently the atom diffracts, but no interference is observed in the far field.

Suppose now that the cavity is present but that no measurement is made on the field after the interaction, so that no path information is obtained. Mathematically this situation is modeled by tracing over the field. The calculation of the far-field distribution is equivalent to adding up the *probability* distributions resulting from all possible field measurements. Because the measurement of any probable value for the amplitude quadrature localizes the atom at one of the two slits, resulting in loss of interference, the sum of the far-field distributions resulting from all such measurements exhibits no interference [see Fig. 12(b)].

In the case where the cavity is present but no field measurement is made we may think of the loss of interference as being due to the *availability* of path information. During the interaction with the standing wave, path information has been encoded in the field, and is available by means of a field measurement. Whether or not we choose to extract the information has no bearing on the physical situation and the interference fringes disappear.

Now suppose that the field amplitude is reduced. As was noted in Sec. III, the resolving power of the scheme increases in proportion to the amplitude of the field. If the field intensity is too low, then a measurement of the

amplitude quadrature cannot distinguish unambiguously which slit the atom passed through [see Fig. 13(a)]. Due to the incompleteness of the path information recorded in the field, partial interference is restored [see Fig. 13(b)].

Instead of thinking of the loss of interference in the presence of the cavity as being due to the availability of *welcher Weg* information, we may attribute it to random momentum kicks suffered by the atom as it scatters from photons in the cavity. A momentum kick will deflect the atom and shift the whole interference pattern across the screen. Random momentum kicks can thereby smear out the interference pattern. The magnitude of the momentum kicks needed to wash out the interference pattern is $2\hbar k$, which is exactly the momentum transferred between the atom and the field during one virtual atomic transition. As the field intensity is reduced, the atom has a lower probability of scattering from a photon in the field, and hence the interference fringes return.

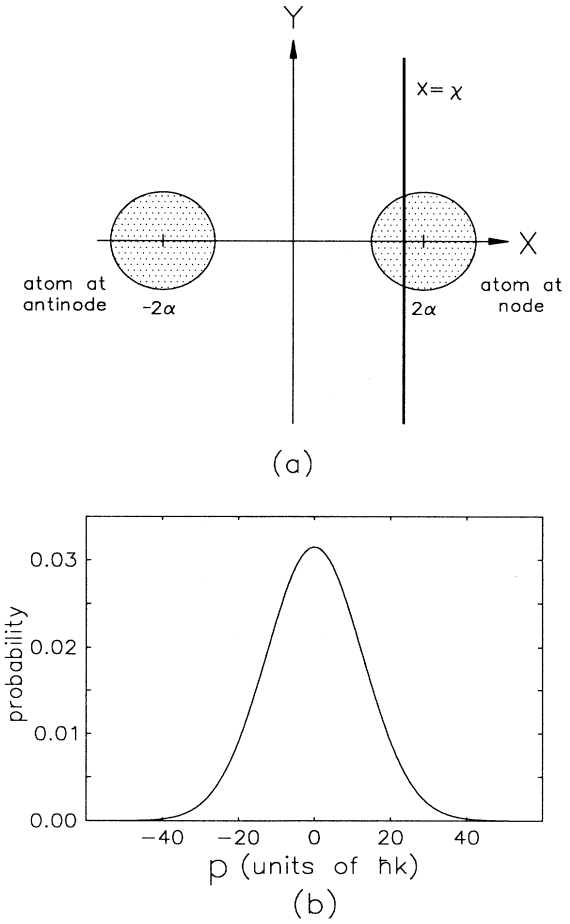

FIG. 12. (a) An atom passing through a node of the standing wave does not affect the field. An atom passing through an antinode of the standing wave changes the phase of the field by π. The path information can be extracted by measuring the amplitude quadrature X of the field. (b) The momentum distribution of the atom after it has passed through a standing wave of initial amplitude $\alpha = \sqrt{8}$ and no field measurement has been made.

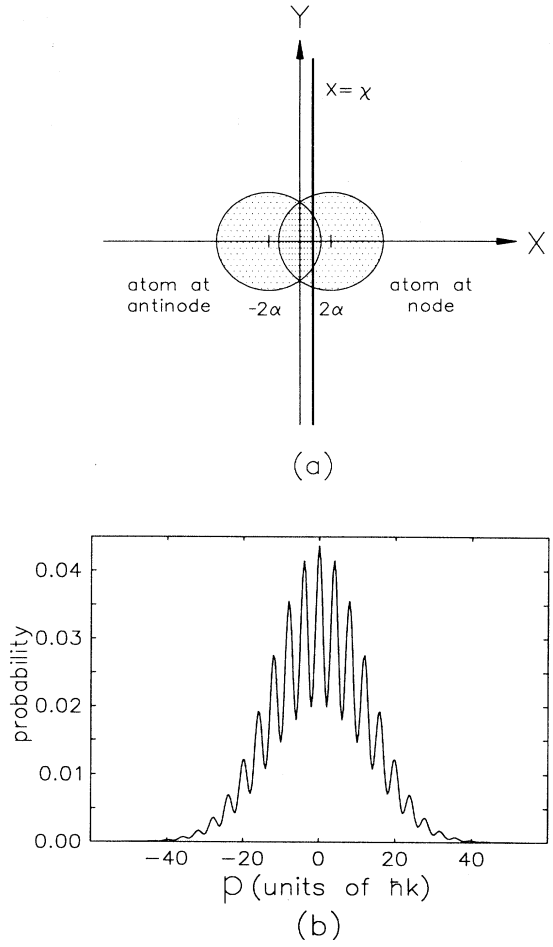

FIG. 13. (a) For a sufficiently low field intensity, the measurement of the amplitude quadrature X cannot determine unambiguously whether the atom passed through a node or an antinode of the standing wave. (b) The momentum distribution of the atom after it has passed through a standing wave of initial amplitude $\alpha = \sqrt{0.5}$ and no field measurement has been made.

B. The quantum eraser

It has been shown that path information about the atom is recorded in the field by the interaction in the cavity. If instead of measuring the amplitude quadrature X of the field after the interaction we choose to measure the phase quadrature Y, no path information is revealed [see Fig. 14(a)]. In fact, the path information is erased permanently, as if by a quantum eraser [16].

Figure 14(b) shows the far-field distribution resulting from two possible measurements of the phase quadrature Y. In each case the *welcher Weg* information is erased, and complete interference is seen in the far field. The position of the fringes depends on the particular value measured for Y, and if the far-field distributions resulting from all possible measurements of Y are summed the resulting "no-measurement" distribution exhibits no interference fringes.

For a sufficiently high field intensity, a measurement of

the amplitude quadrature X can be considered to reveal the particlelike behavior of the atom, because it specifies a unique slit through which the atom passed. On the other hand, a measurement of the phase quadrature Y can be considered to reveal the wavelike behavior of the atom, since the conditional far-field distribution for a particular Y measurement exhibits interference. The experimentalist may delay the decision as to display wavelike or particlelike behavior until after the atom-field interaction, when the atom can no longer be physically manipulated.

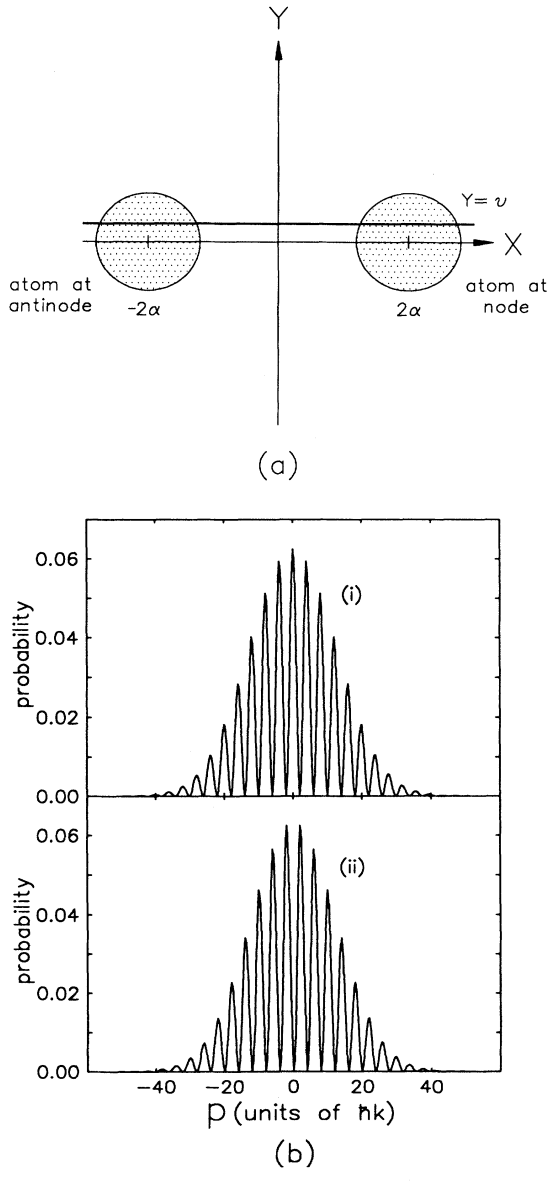

FIG. 14. (a) No path information is revealed by a measurement of the phase quadrature Y. (b) The momentum distributions resulting from measurements of the phase quadrature Y exhibit complete interference. The interference pattern resulting from the measurement $Y = 0$ (i) is in antiphase with the pattern resulting from the measurement $Y = \pi/2\alpha$ (ii). In these graphs the initial field amplitude is assumed to be $\alpha = \sqrt{8}$.

VII. EXPERIMENTAL IMPLEMENTATION

The main difficulty in implementing the position localization scheme experimentally is finding a setup in which atom-field coupling processes dominate the cavity and atomic relaxation in the system evolution. This is possible using Rydberg atoms in a microwave cavity, and has recently been achieved with a high-finesse optical microcavity [17]. The usable parameter regime is determined by the following operating conditions.

Condition 1: The Raman-Nath condition

The transverse distance Δx traveled by the atom during the interaction must be negligible:

$$\Delta x \ll \lambda. \tag{40}$$

Δx can be estimated using the relation $\Delta x = \Delta p\, t/2m$, where t is the interaction time and Δp is the momentum gained by the atom after it has scattered from photons in the cavity for time t. Δp increases with the number of photons in the cavity $\langle n \rangle$ and the momentum per photon

$$\Delta p = \eta \langle n \rangle \hbar k. \tag{41}$$

The constant of proportionality η characterizes the number of times that the atom scatters from each photon during the interaction. It is found numerically to be approximately independent of field strength and to have a value of $\eta \approx 5$.

Condition 2: High detuning

The detuning $\Delta = \omega_0 - \omega_a$ of the atomic transition frequency from the cavity frequency must be sufficiently high that the population of the atomic excited state remains small during the interaction. This condition is satisfied provided

$$\Delta^2 \gg 4\langle n \rangle |g|^2. \tag{42}$$

Condition 3: $t \ll \tau_{\text{cavity}}$

The interaction time was assumed to be much less than the cavity lifetime.

Condition 4: High field intensity

The resolving power increases in proportion to the amplitude of the standing light wave. A field intensity of at least $\langle n \rangle \approx 8$ is required to resolve the atomic position to significantly less than a wavelength.

Condition 5: $|g|^2 t/\Delta \approx \pi$

Under this condition a phase change of about π is induced on the light field when an atom passes through an antinode of the standing wave. This is the optimal phase change.

Condition 6: $\lambda <$ *atomic coherence length*

To obtain interference effects, the wave function of the atom as it enters the cavity must be phase coherent across a width of the order of a wavelength λ of the cavity mode.

The six conditions place conflicting requirements on the experimental parameters, and to satisfy all the conditions simultaneously requires very high atom-field coupling. The Raman-Nath condition is more easily satisfied for low field intensities and short interaction times. However, high field intensities improve the position resolution, and long interaction times are required to induce a measurable phase shift on the radiation field.

Satisfying conditions 1, 2, and 5 simultaneously produces the following restriction on the atom-field coupling:

$$|g| \gg 2\langle n\rangle^{3/2}\left(\frac{\pi^2\eta\hbar}{\lambda^2 m}\right). \tag{43}$$

Because of the inverse square dependence of $|g|$ on the wavelength λ of the standing wave, implementation of the position localization scheme in the optical regime requires extremely high atom-field coupling ($g \gtrsim 10^8$ Hz). The required interaction time is $t \sim 0.1\mu$s. The highest atom-field coupling yet reported is a value of $g = 2\pi(3.2 \pm 0.2)$ MHz obtained by Kimble *et al.* [17] using a high-finesse optical microcavity. The lifetime of Kimble's cavity was $\tau = (0.18 \pm 0.02)\mu$s.

Some flexibility in the choice of parameters is possible if we turn the experimental arrangement used by Sleator *et al.* [3] into a ring cavity. A standing wave of wavelength longer than the photon wavelength is created by reflecting a traveling wave off a mirror at a grazing angle. Increasing the wavelength of the standing wave reduces the value needed for the atom-field coupling $|g|$, but increases the required interaction time by the same factor.

To obtain the diffraction and interference effects predicted in the previous sections, the atomic distribution entering the cavity must be phase coherent across a width of the order of λ. In the optical regime, phase coherence across the required widths is easily achievable by collimation.

The spatial distribution of the atomic beam entering the cavity may be established by a physical slit or a more sophisticated position selection device, but it must have an effective slit width of less than a wavelength of the cavity mode. Material diffraction gratings with a period of 200 nm have been constructed [18]. Slits of this width could be used to implement the scheme in the optical regime. Another possible mechanism for preparing the initial position distribution would be to use a technique such as Raman induced resonance imaging [5].

The far-field diffraction and interference effects predicted in the previous sections should be observable if the scheme is implemented in the optical regime using a microcavity. However, to observe the near-field interference would require a detector placed very close to the cavity with resolution even better than that of the localization scheme presented here. This would be very difficult to achieve in the optical regime.

The spatial dimensions in the problem scale with the wavelength of the light, so that if longer-wavelength radiation is used to implement the scheme, the near-field interference pattern would become larger and therefore easier to observe. However spatial coherence would be required over larger widths in the initial atomic distribution. If atomic coherence lengths of about 100 μm can be achieved, it should be feasible to implement the scheme using Rydberg atoms in a microwave cavity and observe near-field interference, provided that homodyne measurements can be made on the cavity field.

VIII. CONCLUSION

When an atom interacts with a standing light wave in an optical cavity, information about the position of the atom is recorded in the phase of the field. This information may be extracted by making a quadrature phase measurement on the light field.

If the atom enters the cavity with a statistical position distribution, the field measurement provides an indirect classical position measurement of the atom. However, if the atomic distribution is phase coherent across its width, the field measurement produces a quantum localization of the atom, and creates a virtual slit (or slits) from which the atom diffracts, just as it would from a real physical slit.

Particular field measurements may localize the atom so that its wave function collapses to a distribution with multiple peaks located midway between the nodes and antinodes of the standing wave. Every alternate "beam" of the atomic wave function is deflected in the opposite direction. In the near field, atomic interference is predicted between adjacent beams, and in the far-field interference should be observable between alternate beams of the atomic wave function.

If the transverse distribution of the atom before it enters the cavity is sufficiently narrow, a field measurement may produce just one virtual slit. The width of this virtual slit may be varied, either by adjusting the phase of the field quadrature measured or by splitting the beam and thereby altering the resolution of the field measurement. In either case the the atom diffracts just as it would from a real physical slit; the range of scattering angles increases as the width of the virtual slit decreases.

Atomic position information encoded in the standing wave field can be used to provide *welcher Weg* information in a double-slit interference experiment. For the parameters considered here, a measurement of the amplitude quadrature of the field specifies a unique slit through which the atom passed, thus revealing the particle properties of the atom and destroying the interference pattern. A measurement of the phase quadrature erases all path information, thereby recovering the interference

phenomena and displaying the wavelike behavior of the atom.

The central problem in implementing the position localization scheme is achieving a sufficiently high atom-field coupling. This difficulty is overcome in the microwave regime using Rydberg atoms in a microwave cavity, and may be possible in the optical regime using a microcavity. The far-field atomic diffraction and interference effects discussed in this paper should be observable if the scheme can be implemented in the optical regime, and near-field interference should be observable if the scheme can be implemented in the microwave regime.

ACKNOWLEDGMENTS

This research has been supported by the University of Auckland Research Committee, the New Zealand Vice Chancellors' Committee, the New Zealand Lottery Grants Board, IBM New Zealand, and the United States Office of Naval Research.

---

* Permanent address: Department of Physics, University of Auckland, Private Bag 92019, Auckland, New Zealand.

[1] See the special issue on mechanical effects of light, J. Opt. Soc. Am. B **2** (11) (1985) and the special issue on laser cooling and trapping of atoms, J. Opt. Soc. Am. B **6** (11) (1989).

[2] M. J. Holland, D. F. Walls, and P. Zoller, Phys. Rev. Lett. **67**, 1716 (1991).

[3] T. Sleator, T. Pfau, V. Balykin, O. Carnal, and J. Mlynek, Phys. Rev. Lett. **68**, 1996 (1992)

[4] C. Salomon, J. Dalibard, A. Aspect, H. Metcalf, and C. Cohen-Tannoudji, Phys. Rev. Lett. **59**, 1659 (1987).

[5] J. E. Thomas, Phys. Rev. A **42**, 5652 (1990); K. D. Stokes, C. Schnurr, J. R. Gardner, M. Marable, G. R. Welch, and J. E. Thomas, Phys. Rev. Lett. **67**, 1997 (1991).

[6] Pippa Storey, Matthew Collett, and Daniel Walls, Phys. Rev. Lett. **68**, 472 (1992).

[7] H. P. Yuen and J. H. Shapiro, IEEE Trans. Inform. Theory **26**, 78 (1980)

[8] M. A. M. Marte and P. Zoller, Appl. Phys. B **54**, 477 (1992).

[9] Even if no field measurement is made, the atom is diffracted from the intensity grating formed by the standing light wave. See, for example, P. E. Moskowitz, P. L. Gould, S. R. Atlas, and D. E. Pritchard, Phys. Rev. Lett. **51**, 370 (1983).

[10] The focusing effect of the standing wave can be used to create contractive states and beat the standard quantum limit. These results are planned to be discussed in a forthcoming publication.

[11] K. R. Popper, *Quantum Theory and the Schism in Physics* (Hutchinson, London, 1982), pp. 27–29.

[12] M. J. Collett and R. Loudon, Nature **326**, 671 (1987).

[13] E. Arthurs and M. S. Goodman, Phys. Rev. Lett. **60**, 2447 (1988).

[14] C. Y. She, J. Opt. Soc. Am. B **4**, 1727 (1987).

[15] Niels Bohr, Phys. Rev. **48**, 696 (1935).

[16] M. O. Scully and Kai Drühl, Phys. Rev. A **25**, 2208 (1982).

[17] G. Rempe, R. J. Thomas, R. J. Brecha, W. D. Lee, and H. J. Kimble, Phys. Rev. Lett. **67**, 1727 (1991).

[18] D. W. Keith, C. R. Ekstrom, Q. A. Turchette, and D. E. Pritchard, Phys. Rev. Lett. **66**, 2693 (1991).